EPFL

Simulation and Optimization of Urban Traffic Congestion

Rayane El Kasri and Zacharie Maucout

December 18, 2025

1 Deviation from Project Proposal

The initial project proposal focused on comparing traffic lights and roundabouts with respect to pollutant emissions, combining traffic simulation, emission factor models, and atmospheric dispersion. During the early implementation phase, it became clear that this approach involved a level of complexity that was disproportionate to the scope and time frame of the project.

In particular, the limited availability of accessible and well-documented research linking intersection type, microscopic traffic dynamics, and emission models made reliable implementation and validation challenging. Integrating vehicle dynamics, COPERT-based emission factors, and dispersion models would have required strong assumptions and extensive calibration, potentially undermining the robustness of the conclusions.

As a result, we decided to refocus the project on a more tractable yet still highly relevant problem: the simulation of urban traffic congestion and the comparative evaluation of traffic signal control strategies. This revised scope allowed us to concentrate on network-level congestion phenomena, signal control performance, and reproducibility, while maintaining a clear engineering focus and delivering well-supported, interpretable results.

2 Introduction

Urban traffic congestion is a major challenge for modern cities, leading to increased travel times, reduced travel time reliability, and significant environmental and economic costs. As urban demand continues to grow, signalized intersections increasingly act as critical bottlenecks that determine overall network performance.

Traffic signal control plays a central role in regulating vehicle flows and mitigating congestion, particularly under high-demand conditions. While fixed-time signal plans remain widely deployed due to their simplicity, adaptive strategies have been proposed to better respond to spatio-temporal variations in traffic demand.

The objective of this project is to develop a computational traffic model capable of reproducing network-level congestion phenomena and to compare fixed-time and adaptive signal control strategies as traffic demand increases. The study is conducted from the perspective of a client interested in identifying robust control strategies under congested operating conditions.

The central research question addressed in this work is: *How do fixed-time and adaptive traffic signal control strategies compare in their ability to delay congestion and maintain performance as demand increases in an urban network?*

Three control strategies are evaluated: fixed-time control, actuated control, and max-pressure control.

3 Modeling Approach

3.1 Network, Time and Space Discretization

We represent the urban network as a directed graph composed of links connected by signalized intersections. Each link is discretized into a sequence of homogeneous cells (space discretization), and vehicle motion is simulated in discrete time steps (time discretization).

Let $\Delta t = 0.5\,\text{s}$ be the simulation time step. The maximum speed is set to an urban speed limit of $v_{\max} = 50\,\text{km/h} \approx 13.89\,\text{m/s}$. To ensure that vehicles move at most one cell per time step, we set the cell length to:

$$L_{\text{cell}} = v_{\max}\,\Delta t \approx 13.89 \times 0.5 \approx 6.94\,\text{m}.$$

Each cell has a capacity of one vehicle (binary occupancy). For a given lane (or single-lane link), we denote the occupancy of cell i at time step k by

$$x_i(k) \in \{0, 1\}.$$

A queue on an approach is represented by consecutive occupied cells upstream of an intersection.

3.2 Vehicle Movement (Cell Update Rule)

At each time step, vehicles attempt to move forward by one cell, subject to downstream availability. For two consecutive cells $i \rightarrow i+1$ within a link, a vehicle transfer occurs if:

$$x_i(k) = 1 \quad \text{and} \quad x_{i+1}(k) = 0.$$

The update can be expressed as a conservative flow between cells:

$$x_i(k+1) = x_i(k) - f_i(k) + f_{i-1}(k),$$

where the cell-to-cell flow $f_i(k) \in \{0, 1\}$ is defined by:

$$f_i(k) = \begin{cases} 1 & \text{if } x_i(k) = 1 \text{ and } x_{i+1}(k) = 0 \text{ and movement is permitted,} \\ 0 & \text{otherwise.} \end{cases}$$

Within links (non-intersection cells), "movement is permitted" is always true. At intersections, it depends on the traffic signal state (see below).

3.3 Intersection Model and Signal Constraints

An intersection connects incoming approaches to outgoing links via a set of allowed movements (e.g., straight movements in our simplified setting). A movement m is characterized by: - an upstream (approach) queue or last upstream cell, - a downstream receiving cell (first cell of the outgoing link), - a signal permission determined by the active phase.

A vehicle can traverse the intersection on movement m at time k if:

(i) upstream is occupied $\quad \wedge \quad$ (ii) downstream receiving cell is empty $\quad \wedge \quad$ (iii) movement m is green at time k.

Condition (ii) models finite storage and generates *spillback*: when downstream cells are full, upstream vehicles cannot be served even if the signal is green.

3.4 Stochastic Arrivals and Entry Blocking

Vehicles enter the network through entry links. Demand is parameterized by an arrival rate λ expressed in *vehicles per minute per entry*. Internally, we convert to vehicles per second:

$$\lambda_s = \frac{\lambda}{60}.$$

With discrete time, arrivals are implemented as a Bernoulli process per time step with probability:

$$p_{\text{arr}} = \lambda_s \Delta t = \frac{\lambda}{60} \Delta t.$$

At each step, an arrival attempt is generated with probability p_{arr}. The vehicle is inserted if the first cell of the entry link is empty. Otherwise, the arrival is rejected and counted as a *blocked entry*. Formally, if $x_{\text{entry},1}(k) = 1$, then the attempted arrival is blocked.

This mechanism ties demand exceeding capacity to observable spillback/saturation effects through blocked entries.

3.5 Traffic Signal Control Strategies

We evaluate three signal control strategies: fixed-time, actuated, and max-pressure. Each intersection has a finite set of phases Φ, where each phase $\phi \in \Phi$ specifies which movements are granted green simultaneously.

Fixed-time control. A fixed-time controller repeats a cycle of duration C (in seconds), partitioned into green splits for each phase. Let g_ϕ be the green duration allocated to phase ϕ such that $\sum_{\phi \in \Phi} g_\phi = C$

(ignoring lost times for simplicity). The active phase at time t is determined deterministically by the cycle schedule.

Actuated control (local queue-based). Actuated control adjusts green time based on local demand. Let $Q_\phi(k)$ be a proxy for demand under phase ϕ (e.g., sum of queue occupancies on the approaches served by ϕ). The controller keeps the current phase if it remains demanded and a minimum green $g_{\min}$ has been satisfied; otherwise it switches (subject to optional maximum green $g_{\max}$). In simplified form:

$$\text{keep phase } \phi \text{ if } Q_\phi(k) > 0 \text{ and } g_{\min} \leq g_\phi^{\text{elapsed}}(k) < g_{\max}.$$

This provides adaptivity but remains strictly local.

Max-pressure control. Max-pressure selects at each decision point the phase that maximizes a pressure objective based on upstream and downstream congestion. For each movement m allowed by phase ϕ, define: - $q_u(m, k)$: upstream queue measure (e.g., number of occupied cells on the incoming approach for m), - $q_d(m, k)$: downstream congestion measure (e.g., occupancy count on the outgoing link for m).

The pressure of phase ϕ at time k is computed as:

$$P(\phi, k) = \sum_{m \in \mathcal{M}(\phi)} \big(q_u(m, k) - q_d(m, k)\big),$$

where $\mathcal{M}(\phi)$ is the set of movements served by phase ϕ. The controller selects:

$$\phi^*(k) = \arg\max_{\phi \in \Phi} P(\phi, k),$$

subject to basic constraints (e.g., minimum green to avoid excessive switching). Intuitively, this rule favors phases that discharge high upstream queues while avoiding sending flow into already congested downstream links, thereby mitigating spillback and improving network stability.

3.6 Performance Metrics and Computation

We compute complementary metrics capturing efficiency, saturation, and reliability.

Travel time. For each vehicle n, we record entry and exit times $(t_n^{\text{in}}, t_n^{\text{out}})$, and define travel time:

$$TT_n = t_n^{\text{out}} - t_n^{\text{in}}.$$

Mean travel time is $\overline{TT} = \frac{1}{N} \sum_{n=1}^{N} TT_n$, and the P95 travel time is the empirical 95th percentile of $\{TT_n\}$.

Throughput. Over a simulation horizon T (seconds), let N_{out} be the number of vehicles that exited the network. Throughput is:

$$\text{Throughput} = \frac{N_{\text{out}}}{T} \quad \text{(vehicles/s)}.$$

Average queue length. We approximate queue length by counting occupied cells on approach links. If $\mathcal{A}$ is the set of approach cells near intersections, then at time k:

$$Q(k) = \sum_{i \in \mathcal{A}} x_i(k),$$

and the reported average queue length is the time average:

$$\overline{Q} = \frac{1}{K} \sum_{k=1}^{K} Q(k).$$

Blocked entries. Blocked entries count how often an arrival attempt cannot be inserted because the entry cell is occupied. If $B(k)$ is the number of blocked attempts at step k, the total blocked entries is $\sum_k B(k)$, which acts as a direct indicator of saturation and spillback.

Stochastic robustness. Each configuration (controller, demand level) is simulated with multiple random seeds. We report aggregated metrics across seeds to reduce noise and ensure that comparisons reflect systematic performance differences rather than stochastic fluctuations.

4 Experimental Design and Reproducibility

Traffic demand is varied from low to highly congested conditions by sweeping the arrival rate λ from 3 to 30 vehicles per minute per entry. This range allows the exploration of both free-flow and saturated regimes, including conditions beyond the effective network capacity.

For each demand level, all three control strategies are evaluated using identical network configurations and random seeds. The full experimental pipeline is automated, including simulation execution, result aggregation, and figure generation, ensuring reproducibility from the submitted code repository.

5 Results

5.1 Queue Growth and Congestion Formation

Figure 1a shows that average queue length increases monotonically with the arrival rate for all control strategies, but with markedly different growth rates.

At low demand ($\lambda = 3$ veh/min/entry), average queues remain small: approximately 2.3 veh for fixed-time and actuated control, and below 1 veh for max-pressure. As demand increases to $\lambda = 12$, fixed-time control already accumulates queues close to 10 veh, whereas actuated control remains near 5.2 veh and max-pressure near 4.2 veh.

Beyond $\lambda = 18$, congestion accelerates. At $\lambda = 21$, average queues reach approximately 14.4 veh under fixed-time, 12.9 veh under actuated control, and 9.6 veh under max-pressure. For $\lambda \geq 0 \, 24$, queues approach a plateau around 14–15 veh for fixed-time and 13–13.5 veh for adaptive controllers, reflecting saturation of network storage and widespread spillback.

5.2 Network Saturation and Spillback

The number of blocked entries (Figure 1b) remains negligible up to $\lambda \approx 0 \, 12$, with fewer than 1 000 blocked entries across all strategies. A sharp non-linear increase is observed beyond $\lambda = 15$.

At $\lambda = 18$, blocked entries reach approximately 2 600 for fixed-time control, compared to 2 000 for actuated and 1 900 for max-pressure. The divergence becomes pronounced at $\lambda = 21$: fixed-time exceeds 6 500 blocked entries, actuated reaches around 4 200, while max-pressure remains below 2 700.

At the highest demand level ($\lambda = 30$), blocked entries rise to nearly 19 500 under fixed-time control, 17 000 under actuated control, and approximately 13 000 under max-pressure, confirming that max-pressure significantly delays and mitigates spillback under extreme congestion.

5.3 Travel Time and Reliability

Mean travel time results (Figure 1c) show clear separation between control strategies as demand increases. At arrival rate $\lambda = 3$, all strategies yield comparable travel times between 85 s and 135 s. As demand reaches arrival rate $\lambda = 12$, fixed-time control increases to approximately 157 s, while actuated control drops to 109 s, and max-pressure remains below 100 s.

A sharp degradation occurs beyond $\lambda = 18$. At $\lambda = 21$, mean travel time reaches roughly 234 s for fixed-time control and 194 s for actuated control, while max-pressure remains lower at approximately 122 s. At $\lambda = 30$, mean travel times stabilize around 245 s (fixed-time), 218 s (actuated), and 192 s (max-pressure).
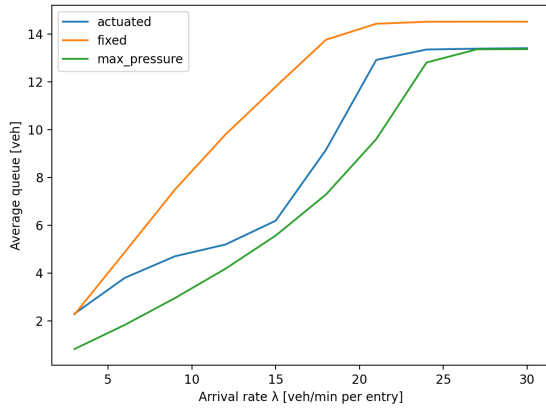
Reliability differences are even more pronounced in the P95 travel time (Figure 1d). At $\lambda = 21$, P95 travel time exceeds 310 s under fixed-time control, compared to 268 s for actuated control and 167 s for max-pressure. At $\lambda = 30$, P95 travel times reach approximately 325 s, 292 s, and 250 s respectively, highlighting the superior robustness of max-pressure in limiting extreme delays.
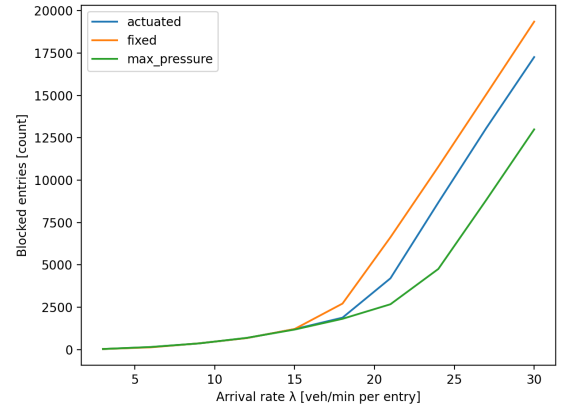
5.4 Throughput and Network Capacity

Throughput results (Figure 2) initially increase linearly with arrival rate. Up to $\lambda = 15$, all strategies exhibit nearly identical throughput, reaching approximately 5.6 veh/s.

Beyond this point, a capacity plateau emerges. Fixed-time control saturates first, stabilizing around 6.4–6.5 veh/s from $\lambda = 18$ onward. Actuated control reaches a higher plateau near 7.1 veh/s, while max-pressure achieves the highest sustained throughput at approximately 8.2 veh/s for $\lambda \geq 0$ 24.
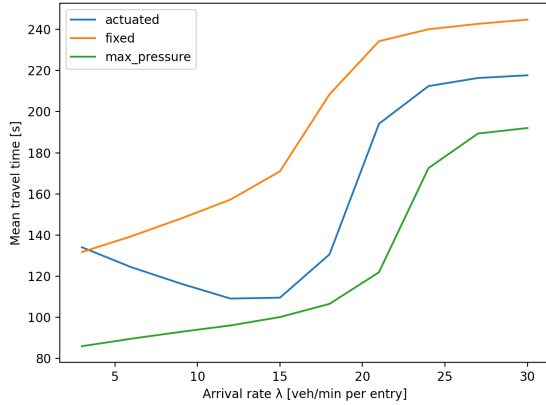
This confirms that, although increasing demand beyond saturation does not increase throughput, control strategies significantly influence the effective network capacity and the severity of congestion-related side effects.
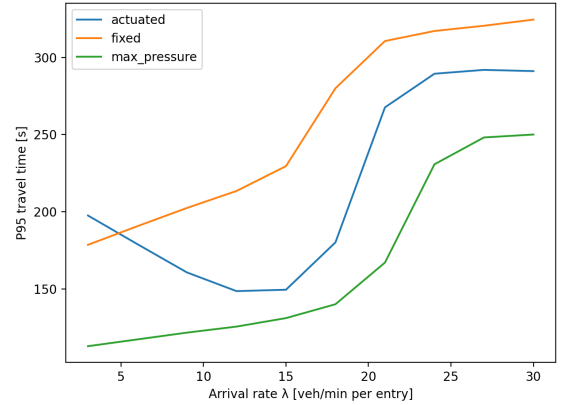

(a) Average queue length.

(b) Blocked entries (spillback).

(c) Mean travel time.

(d) P95 travel time.

Figure 1: Congestion formation and travel time reliability under three signal control strategies.
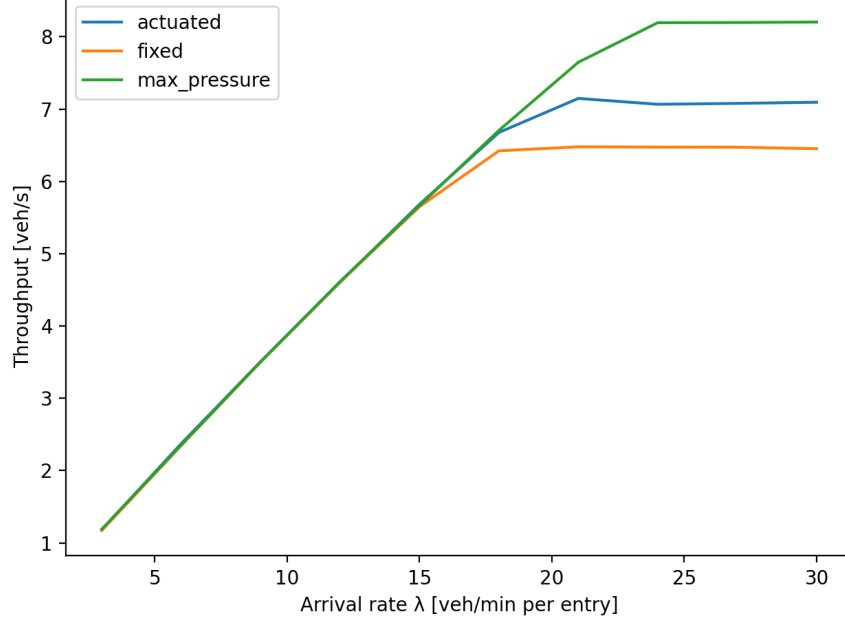
Figure 2: Throughput versus arrival rate. A capacity plateau is observed beyond saturation.

6   Discussion

The results reveal a clear transition from free-flow to saturation as traffic demand increases. Fixed-time control consistently reaches congestion earlier, with faster queue growth and the earliest rise in blocked entries. This behavior reflects the limitations of pre-timed signal plans, which cannot reallocate green time when demand patterns fluctuate spatially or temporally.

Actuated control improves performance at moderate demand levels, consistent with its local responsiveness to traffic conditions. However, once the network approaches saturation, local decisions are insufficient to prevent system-wide spillback effects, leading to rapid deterioration in travel times and reliability.

Max-pressure control consistently outperforms the other strategies across all congestion-related metrics. By prioritizing movements with the highest pressure imbalance, it better balances queues across the network, reduces spillback, and significantly improves travel time reliability, particularly under high demand. Throughput results further confirm that max-pressure control increases the effective capacity of the network, although congestion remains unavoidable once physical storage and discharge limits are reached.

These findings emphasize that congestion evaluation should not rely on throughput alone. Beyond the capacity plateau, user experience continues to degrade through increased delays and reduced reliability. Metrics such as blocked entries and high-percentile travel times are therefore essential to capture spillback dynamics and equity-related impacts under congested conditions.

7   Model Validation and Limitations

Sanity checks confirm internal consistency: under low demand, travel times remain close to free-flow values; results are reproducible across identical random seeds; and congestion indicators increase monotonically with demand.

The model relies on simplifying assumptions, including homogeneous demand, no turning movements (which simplifies conflict patterns and isolates the impact of signal control on network-level congestion) and simplified vehicle interactions. While these assumptions limit realism, they do not affect the comparative conclusions between control strategies.

8   Conclusion and Outlook

This project demonstrates that adaptive traffic signal control strategies substantially improve network robustness and delay the onset of congestion compared to fixed-time control. Among the evaluated strategies, max-pressure control achieves the best overall performance, notably reducing spillback, improving travel time reliability, and increasing the effective network capacity.

Despite these improvements, congestion remains unavoidable once physical capacity limits are reached, highlighting the fundamental constraints of signal control alone. Future work could incorporate turning movements, heterogeneous demand patterns, and corridor coordination strategies (e.g., green waves) to increase realism and enable more deployment-oriented conclusions.

References

[1] P. Varaiya, "The Max-Pressure Controller for Arbitrary Networks of Signalized Intersections," *Advances in Dynamic Network Modeling in Complex Transportation Systems*, 2013.

[2] R. P. Roess, E. S. Prassas, and W. R. McShane, *Traffic Engineering*, 4th ed., Pearson, 2010.

[3] C. F. Daganzo, "The cell transmission model, part II: Network traffic," *Transportation Research Part B*, vol. 29, no. 2, pp. 79–93, 1995.

[4] L. Tassiulas and A. Ephremides, "Stability properties of constrained queueing systems and scheduling policies," *IEEE Transactions on Automatic Control*, vol. 37, no. 12, pp. 1936–1948, 1992.

[5] OpenAI, *ChatGPT (GPT-4) language model*, Used as a writing assistance and research guidance tool, 2025.